

Introduction: Impact craters observed on the surface of Mars give us an important information about the geologic history of the planet. For example, crater size-frequency distribution allows us to estimate retention age of specific areas, extent and morphology of fluidized ejecta blankets reflect (at least, qualitatively) the presence of ice/water in upper layers of Martian crust. At the same time the presence of ice water in target rocks should influence also crater morphology and morphometry. However, the conversion of observed details of impact structures demands better knowledge of cratering mechanics in Martian rocks. The presented project is aimed to make a review of possible mechanical properties of near surface Martian rock. Plausible hypothesis about mechanical properties should facilitate the analysis of observational data on Martian impact craters, especially if one use the technique of computer numerical modeling of impact cratering.

Upper crust as a target for impact cratering: The upper crust of Mars is assumed to be brecciated during the late heavy bombardment period. The brecciated autochthon rocks may be covered by ejecta, volcanic, aeolian, and, in some areas, by marine/lake sediments. Porous space in all rocks, listed above, may be filled with water (brine) and water ice depending on the local pressure-temperature conditions.[1] The cratering mechanics depends on target density, compressibility, initial strength of material, and dissipative properties (internal friction, effective viscosity) of fragmented material, involved into a crater-forming motion. The presence of ice in some layers of target rocks open a possibility to influence cratering in two opposite directions: low-temperature ice in permafrost layers increase the porous rock strength, while possible shock melting of ground ice make, in general, result in the strength/friction decrease. Below we make a draft of a scheme to construct initial conditions for the formation of impact craters of various diameter in different geologic provinces of Mars.

Temperature and pressure gradient: Unknown Martian heat flux is commonly estimated as $\sim 30 \text{ mW m}^{-2}$ [1]. With a lot of assumptions the heat conductivity may be estimated as $\sim 2 \text{ W m}^{-2} \text{ K}^{-1}$ [1]. The resulted near-surface thermal gradient is estimated as $\sim 15 \text{ K km}^{-1}$. Simple pressure estimate give $p = \rho g z \sim 9.3 \text{ Mpa}$ ($\sim 93 \text{ bar}$) for depth z of 1 km (assuming density $\rho \sim 2500 \text{ kg m}^{-3}$ at gravity $g = 3.72 \text{ m c}^{-2}$). Hence the range of pressures along in the assumed porous space of the upper 10 km of Martian crust [1] is growing from atmospheric pressure at the surface to $\sim 100 \text{ Mpa}$ (1 kbar). The temperature

grows up from the surface mean annual value (~ 150 to 170 K at high latitudes and 210 to 220 K at low latitudes) at $+150 \text{ K}$ approximately.

Water/ice content: According to the model of hydrosphere [1] one can list possible variation of the saturation state of porous rocks: (i) upper layer, filled with ice which exist only in high latitudes (low T , low ambient pressure); (ii) dry (desiccated) layers in low latitudes; (iii) water saturated low horizons (T above freezing point of water/brine); (iv) possible intermediate layer of dry porous rocks if the total water column does not fill all the porous space. The model [1] assumes 100% saturation in layers (i) and (iii). One should have reasonable estimates of rock strength for all listed layers before to start any modeling. For dry porous material one can use a numerous experimental data for terrestrial rocks. As an example the shear strength of basalt specimens in triaxial tests is presented in Fig. 1.

Ice strength: Shear strength data for pure ice are presented in Figs. 2-4. The strain rate dependence of strength as well as structure of ice result in relatively large data scatter. However it is evident that the ice strength grow approximately 5 to 10 times when temperature decrease from melting point to $\sim 150 \text{ K}$. For lower temperatures the strength is approximately constant.

Permafrost strength: The permafrost strength depends on temperature (being larger at low temperatures) and size-frequency distribution of rock/soil particles reflecting available particle surface absorbing (unfrozen) water. In general the permafrost strength follow the ice strength trend. For many materials strength is 1.5 to 2 times above the pure ice strength at the same temperature. After failure broken material behave as Coulomb material with a friction coefficient depending on ice content (i.e. on the rock porosity). For high ice content the friction is close to pure ice friction which is \sim twice less than general rock dry friction. For stress state invariants of shear $T_s = \{[(\sigma_1 - \sigma_2)^2 + (\sigma_1 - \sigma_3)^2 + (\sigma_2 - \sigma_3)^2]/6\}^{1/2}$ and pressure $p = (\sigma_1 + \sigma_2 + \sigma_3)/3$ the friction coefficient (T_s/p) for rocks is of ~ 0.7 , while for pure ice it is of ~ 0.5 (at low p) to ~ 0.2 (for $p \geq \sim 20 \text{ MPa}$) [2,3]. However for large strain and strain rate the dynamic friction of ice is a complicated dynamic process, possibly with shear melting (e.g. [4]).

Perspectives: The compiled data shown in Figures allow us to construct a set of possible model targets for Martian impact cratering. Depending on latitude, assumed change with depth of porosity, one can present these targets as layers, where the initial strength is controlled by presence or absence of ice below freezing point and presence/absence of water

saturated fractured rocks in upper ~10 km of Martian crust. It should improve previously published models (e.g. [5]) where dynamic strength of Martian crust assumed to be constant (10 to 20 MPa).

References. [1] Clifford, S. M. (1993) *Journal of Geophysical Research* 98.10973. [2] Beeman, M., et al. (1988) *Journal of Geophysical Research* 93.7625-7633. [3] Sammonds, P. R., et al. (1998) *Journal of Geophysical Research* 103.21795-21816. [4] Oksanen, P. and Keinonen, J. (1982) *Wear* 78.315-324. [5] Stewart, S. T., et al. (2003) in *Shock Compression of Condensed Matter-2003*, 1-4. [6] Byerlee, J. D. (1978) *Pure and Applied Geophysics* 116.615-626. [7] Durham, W. B., et al. (1988) in *Solar System Ices*, 63-78. [8] Singh, S. K. and Jordaan, I. J. (1996) *Cold Regions Science and Technology* 24.153-165.

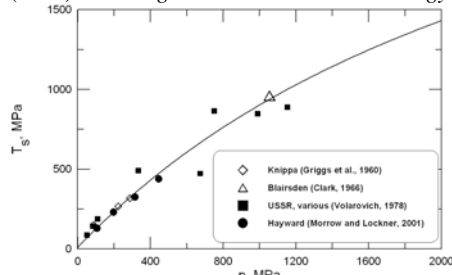


Fig. 1. Shear strength of initially intact basalt specimen in triaxial tests. One can assume that after brittle failure strength of fragmented material is controlled by dry friction (Bayerly law [6]).

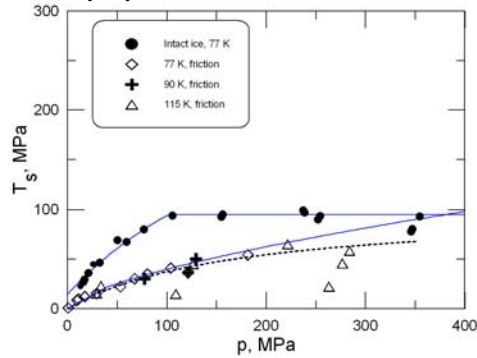


Fig. 2. Low-temperature ice shear strength (black dots) and friction (compressive strength of specimens with a fracture) [2,7].

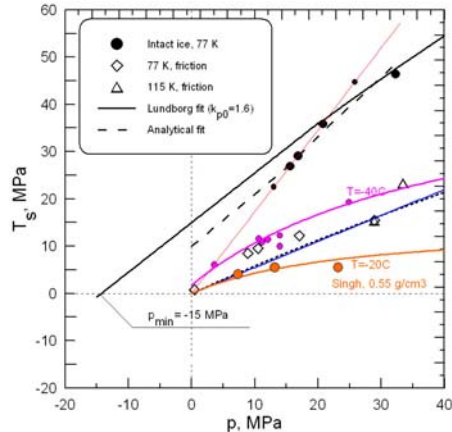


Fig. 3. Low pressure range of data shown in Fig. 1 with the addition of data for large temperatures ([3] for -40 °C, pink; [8] for -20 °C, crashed ice).

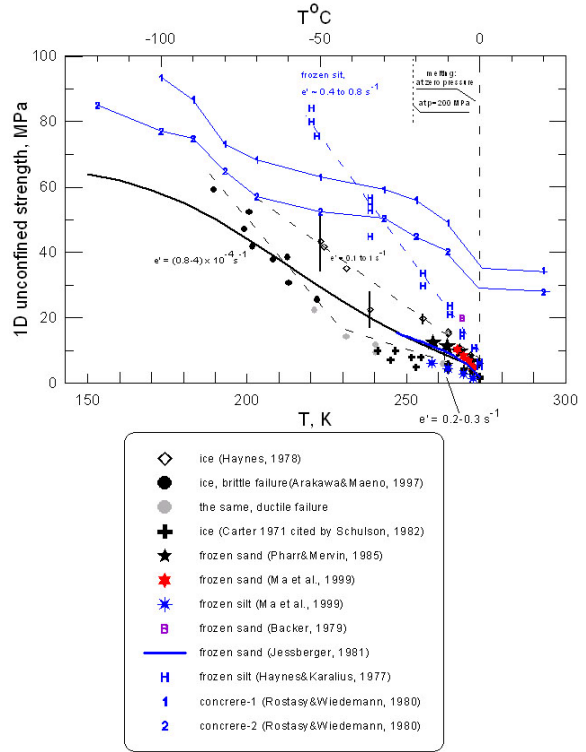


Fig. 4. Unconfined 1D strength of ice and frozen sand, silt, and concrete samples as a function of temperature. At temperatures of ~220K (-50C) frozen silt may be stronger than frozen concrete.

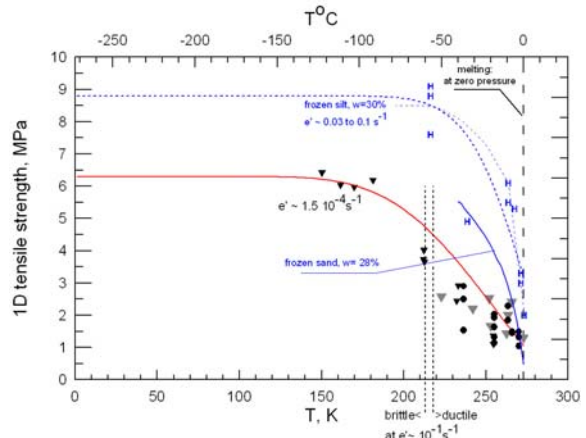


Fig. 5. Tensile strength of ice and permafrost specimens dependence on temperature for most fast tests. Black and gray symbols are for pure ice. Blue symbols and curves are for permafrost.